ELSEVIER

Journal of Fluids and Structures 19 (2004) 1141–1153

JOURNAL OF FLUIDS AND STRUCTURES

www.elsevier.nl/locate/jnlabr/yjfls

A numerical modelling of stator–rotor interaction in a turbine stage with oscillating blades

V.I. Gnesin[a,*], L.V. Kolodyazhnaya[a], R. Rzadkowski[b]

[a]*Department of Aerohydromechanics, Institute of Mechanical Engineering Problems, National Academy of Sciences of Ukraine, 2/10 Pozharsky St., Kharkov 61046, Ukraine*

[b]*Department of Dynamics of Machines, Institute of Fluid Flow Machinery, Polish Academy of Sciences, J. Fiszera St.,14, Gdansk 80 952, Poland*

Received 18 October 2002; accepted 21 July 2004

Abstract

In real flows unsteady phenomena connected with the circumferential non-uniformity of the main flow and those caused by oscillations of blades are observed only jointly. An understanding of the physics of the mutual interaction between gas flow and oscillating blades and the development of predictive capabilities are essential for improved overall efficiency, durability and reliability. In the study presented, the algorithm proposed involves the coupled solution of 3D unsteady flow through a turbine stage and the dynamics problem for rotor-blade motion by the action of aerodynamic forces, without separating the outer and inner flow fluctuations. The partially integrated method involves the solution of the fluid and structural equations separately, but information is exchanged at each time step, so that solution from one domain is used as a boundary condition for the other domain. 3-D transonic gas flow through the stator and rotor blades in relative motion with periodicity on the whole annulus is described by the unsteady Euler conservation equations, which are integrated using the explicit monotonous finite volume difference scheme of Godunov–Kolgan. The structural analysis uses the modal approach and a 3-D finite element model of a blade. The blade motion is assumed to be constituted as a linear combination of the first natural modes of blade oscillations, with the modal coefficients depending on time. A calculation has been done for the last stage of the steam turbine, under design and off-design regimes. The numerical results for unsteady aerodynamic forces due to stator–rotor interaction are compared with results obtained while taking into account blade oscillations. The mutual influence of both outer flow non-uniformity and blade oscillations has been investigated. It is shown that the amplitude-frequency spectrum of blade oscillations contains the high-frequency harmonics, corresponding to the rotor moving past one stator blade pitch, and low-frequency harmonics caused by blade oscillations and flow non-uniformity downstream from the blade row; moreover, the spectrum involves the harmonics which are not multiples of the rotation frequency.

1. Introduction

The problem of unsteady flows in aerodynamic cascades arouses considerable interest mainly because of the effect of non-stationarity on the optimal designs, efficiency and reliability of turbomachine operation. The energy transfer in a

*Corresponding author.
E-mail addresses: gnesin@ipmach.kharkov.ua (V.I. Gnesin), z3@imp.gda.pl (R. Rzadkowski).

0889-9746/$ - see front matter © 2004 Elsevier Ltd. All rights reserved.
doi:10.1016/j.jfluidstructs.2004.07.001

turbine stage is accompanied by interaction of aerodynamic, inertial and elastic forces acting on the blades, which can cause excessive blade vibration, leading to structural fatigue failures. The mutual interaction of these forces while taking into account the structural and mechanical damping determines the aeroelastic behaviour of the blades and represents an important problem of reliability and safety.

Because of the extreme complexity of the full problem, formerly the hypothesis was accepted that blade vibrations cause unsteady effects, which are significantly smaller than unsteady effects due to flow non-uniformity upstream and downstream of the blade row. In other words, it was assumed that there is no feedback of blade motion on the flow. This incorrect, in most cases, assumption turned out to be a very fruitful one, as it allowed to uncouple the two physical domains and to achieve great advances in each of them (namely in the unsteady aerodynamics and forced response aspects). Since the beginning of the 1980s there has been a great deal of work on numerical methods for the calculation non-linear unsteady flows by time-marching methods. These procedures have been carried out in particular in connection with flows through aerodynamically coupled blade rows. Some assume inviscid flow and use the Euler equations (Gnesin, 1982; Koya and Kotake, 1985; Rao and Delancy, 1990), while others adopt the Navier–Stokes equations with turbulence modelling, such as Yershov et al. (2001). It is clear that in spite of a number of limitations in the non-linear time-marching methods, particularly for 3-D viscous calculations, these have given us very useful tools to investigate a whole variety of different kinds of unsteady flows, including stator/rotor interaction, rotating stall, etc.

The incorrectness of the hypothesis concerning the insignificant influence of oscillating blades on the flow is proved by the fact that uncoupling of the two domains results in the exclusion from consideration of a particularly difficult problem in turbomachinery aeroelastic phenomena, namely that of self-excited oscillations (flutter) or auto-oscillations. These phenomena are characterized by instability, continuous interaction and energy exchange between the fluid and the structure; so, they cannot be studied properly in the frame of each of uncoupled domains separately (aerodynamics or structural dynamics).

The traditional approach in flutter calculations of bladed disks is based on frequency domain analysis (Bakhle et al., 1992; Bolcs and Fransson, 1986), in which the blade motion is assumed to be a harmonic function of time with a constant phase lag between adjacent blades, and the natural mode shapes and frequencies are obtained by in-vacuum structural computations. This approach ignores the feedback effect of the fluid on structural vibration.

At present the existing approaches in flutter calculations of 3-D blade rows use the simultaneous integration in time of the equations of motion for the structure and the fluid (Chew et al., 1998; Gnesin and Kolodyazhnaya, 1999; Gnesin et al., 2000). However, in these works it is supposed that perturbations in the flow are due to blade motion, and the flow far upstream and downstream from the blade row contains small fluctuations of the uniform free-stream.

The aim of the present work is to present the mathematical model and the numerical analysis of the coupled fluid–structure solution for 3-D flow through the turbine stage while taking into account the blade oscillations, but without separating the outer excitation and unsteady effects due to blade motion. This paper includes the numerical results for aeroelastic behaviour of a steam turbine last stage with rotor blades of 760 mm. The mutual influence of both outer flow non-uniformity (upstream and downstream from the blade row) and blade oscillation is investigated.

2. Coupled fluid–structure problem

Aeroelasticity is a multidisciplinary subject combining unsteady aerodynamics and structural dynamics. The simultaneous integration in time of the equations of motion for the fluid and structure in a turbine stage allows the correct assessment of the energy exchange which can occur with the transfer of energy from the mean flow to the moving blade (self-excited oscillations, or flutter), with dissipation of the vibrating blade energy in the flow field (aerodamping) or with a balance between input energy and dissipation (auto-oscillatons or limit-cycle oscillations).

In this study, the partially integrated method is used to solve a coupled aeroelasticity problem for a turbine stage. It involves the solution of the fluid and structural equations separately, but information is exchanged at each time step, so that the solution from one domain is used as a boundary condition for the other domain. In other words, a new rotor blade position is calculated at each time step using the aerodynamic forces at the previous time step, and this new position is used as the new fluid–structure boundary for the next time step when the aerodynamic forces are computed. The simultaneous-sequential integration in time of the equations of motion for the structure and the fluid allows the correct assessment of energy transfer in the turbine stage and blade motion by the action of aerodynamic forces, while taking into account the mechanical and aerodamping.

The aerodynamic and structural models are described in what follows.

2.1. Aerodynamic model

Three-dimensional (3-D) transonic flow of inviscid non-heat-conductive gas through an axial turbine stage is considered in the physical domain, including the nozzle cascade (NC) and the rotor wheel (RW), rotating with constant angular velocity. Taking into account the flow non-periodicity from blade to blade (in the pitchwise direction), it is convenient to choose the calculated domain including all blades of the NC and RW assembly, entry region, axial clearance and exit region (Fig. 1).

Let the stator and the rotor involve z_s and z_r blades, respectively. It is obvious that at each time moment the flow structure in the stage has spatial periodicity with minimal angular stage pitch $T_{\min}$ (in radians), which is defined as $T_{\min} = [2\pi/(z_s - z_r)](k_1 - k_2)$, where k_1 and k_2 are mutually simple natural numbers, proportional to z_s and z_r, respectively ($z_s{:}z_r = k_1{:}k_2$).

Hence, the calculated domain has expansion $T_{\min}$ in the pitchwise direction and involves k_1 interblade channels of the stator cascade and k_2 interblade channels of the rotor wheel. The difference grid is divided into $(k_1 + k_2)$ difference segments; each of them includes a blade and has an expansion in the circumferential direction, which is equal to the pitch of stator or rotor blades, respectively (Fig. 1).

In turn, each of the passages is discretized using a hybrid H–H-grid. The external H-grid remains immobile during the calculation, while the H-internal grid is rebuilt in each iteration by a given algorithm. Therefore, the external points remain fixed, but internal points (points on the blade surface) move according to the blade motion. A fragment of the deforming grid at the middle section of the rotor interblade passage is shown in Fig. 2.

The equations for the spatial transonic flow, including in the general case strong discontinuities in the form of shock waves and wakes behind the exit edges of blades, are written in the relative Cartesian coordinate system rotating with constant angular velocity $\bar{\omega}$, according to the full non-stationary Euler equations, presented in the form of integral conservation laws of mass, impulse and energy (Gnesin and Kolodyazhnaya, 1999):

$$\frac{\partial}{\partial t}\int_{\Omega} f \,\mathrm{d}\Omega + \oint_{\sigma} \vec{F}\cdot\vec{n}\,\mathrm{d}\sigma + \int_{\Omega} H \,\mathrm{d}\Omega = 0, \tag{1}$$

where

$$f = \begin{bmatrix} \rho \\ \rho v_1 \\ \rho v_2 \\ \rho v_3 \\ E \end{bmatrix}; \quad \vec{F} = \begin{bmatrix} \rho\vec{v} \\ \rho v_1\vec{v} + \delta_{1i}p \\ \rho v_2\vec{v} + \delta_{2i}p \\ \rho v_3\vec{v} + \delta_{3i}p \\ (E+p)\vec{v} \end{bmatrix};$$

$$H = \begin{bmatrix} 0 \\ \rho a_{e1} - 2\rho\omega v_2 \\ \rho a_{e2} + 2\rho\omega v_1 \\ 0 \\ 0 \end{bmatrix}; \quad \delta_{ji} = \begin{cases} 1 j = i, \\ 0 j \neq i. \end{cases}$$

Here f is the solution vector, $\vec{F}$ is the inviscid flux through the lateral area σ bounding the finite volume Ω, and H is source vector which contains the terms due to the rotation of the coordinate system, p and ρ are the pressure and density, v_1, v_2, v_3 are the velocity components, a_{e1} and a_{e2} are the transfer acceleration projections, ω is the rotational angular velocity, $E = \rho[\varepsilon + \frac{1}{2}(v_1^2 + v_2^2 + v_3^2 - r^2\omega^2)]$ is the total energy of volume unit, r is the distance from rotation axis, ε is an internal energy of mass unit. The above system of equations is completed by the perfect gas equation $p = \rho\varepsilon(\chi - 1)$, where χ denotes the ratio of the fluid specific heats.

The discretized form of Eqs. (1) was obtained for an arbitrary moving grid following Godunov's idea (Godunov et al., 1976), but in more universal form, extended to three spatial coordinates:

$$\begin{aligned} &\frac{1}{\Delta t}\left[f^{i+\frac{1}{2},j+\frac{1}{2},k+\frac{1}{2}} \cdot \Omega^{i+\frac{1}{2},j+\frac{1}{2},k+\frac{1}{2}} - f_{i+\frac{1}{2},j+\frac{1}{2},k+\frac{1}{2}} \cdot \Omega_{i+\frac{1}{2},j+\frac{1}{2},k+\frac{1}{2}}\right] \\ &\quad + [-(f\sigma w_n)_{i+1} + (f\sigma w_n)_i - (f\sigma w_n)_{j+1} + (f\sigma w_n)_j \\ &\quad - (f\sigma w_n)_{k+1} + (f\sigma w_n)_k] + [F_1\sigma_{i+1} - (F_1\sigma)_i \\ &\quad + (F_2\sigma)_{j+1} - (F_2\sigma)_j + (F_3\sigma)_{k+1} - (F_3\sigma)_k] \\ &\quad + H_{i+\frac{1}{2},j+\frac{1}{2},k+\frac{1}{2}} \cdot \Omega_{i+\frac{1}{2},j+\frac{1}{2},k+\frac{1}{2}} = 0. \end{aligned} \tag{2}$$

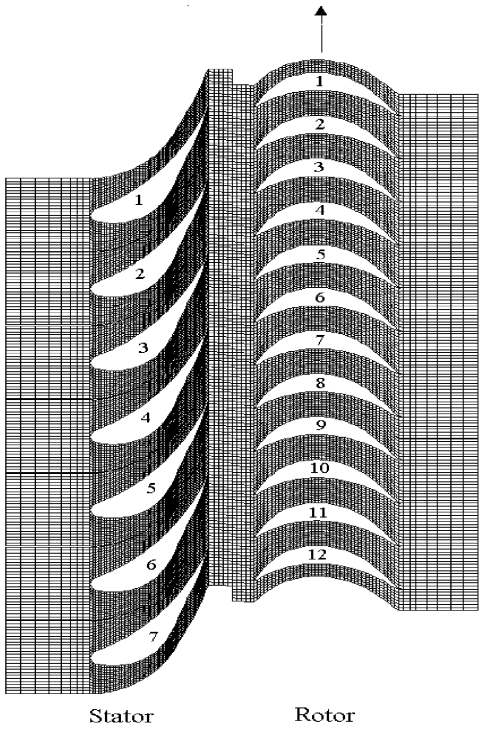

Fig. 1. The tangential root plane of the turbine stage.

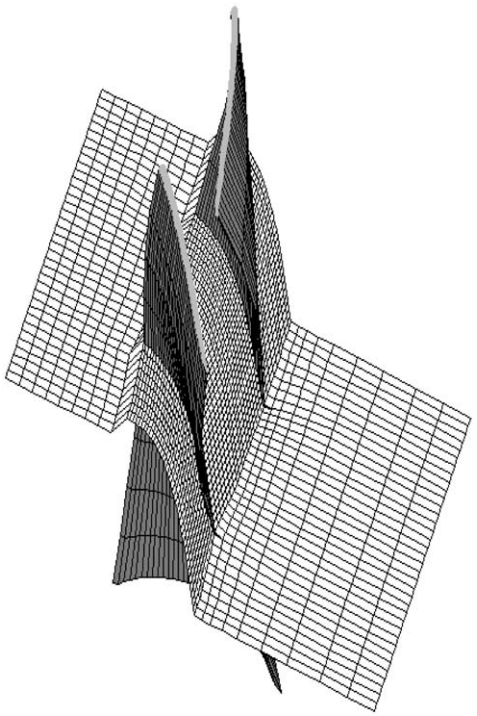

Fig. 2. Fragment of the moving grid for the rotor blade passage.

Here subscripts and superscripts correspond to "old" and "new" cells, f are "small" values in cell centres, F_1, F_2, F_3 are "big" values on the "middle" cell interface, σ and w_n are the area and normal velocity of the "middle" cell interface, respectively. The gasdynamic parameters on the lateral sides (expressions in square brackets with integer indices) are defined from the solution of the problem about the break-down (Riemann problem) of an arbitrary discontinuity on the moving interfaces between two adjacent cells and by using the iteration process.

The difference scheme proposed supposes a piecewise linear distribution of parameters in grid cells. The derivatives for linear extrapolation of gasdynamic parameters inside of cell are calculated with the use of the minimal value of the derivative principle (Gnesin, 1999). Such a way of choosing the derivatives provides a small "spreading" of parameter break-down and eliminates the possibility of appearance of negative values of pressure in the linear approximation. The values obtained for the derivatives are applied to calculate the parameters at the side centers, which in turn are used to calculate the problem about the break-down of discontinuity.

Constructed in this way, the difference scheme is a monotonic scheme, and it has second-order accuracy on the smooth solutions with respect to spatial coordinates and is a first-order approximation with respect to the time coordinate. To increase the approximation order with respect to the time coordinate, it is necessary that the linear approximation of parameters by spatial coordinates should be completed with a linear approximation in time from cell centre to side centre.

It is assumed that the unsteady flow fluctuations are due to both rotor-wheel rotation and to prescribed blade motions, and the flows far upstream and far downstream from the blade row contain at most small perturbations of a uniform free-streams. So, the boundary conditions formulation is based on one-dimensional theory of characteristics. In the general case, when the axial velocity is subsonic, at the inlet boundary, initial values for total pressure, total temperature and flow angles are given, while at the outlet boundary only the static pressure has to be imposed.

The total system of boundary conditions can be represented in the following form.

Before stator:

$$\begin{aligned} &T_0 = T_0(x,y), \quad p_0 = p_0(x,y),\\ &\alpha = \alpha(x,y), \quad \gamma = \gamma(x,y),\\ &d\left(v_3 - \frac{2a}{\chi - 1}\right) = 0. \end{aligned} \tag{3}$$

Behind rotor:

$$\begin{aligned} &p = p(x,y),\ \mathrm{d}p - a^2\mathrm{d}p = 0,\\ &\mathrm{d}v_1 - (\omega^2 r - 2\omega v_2)\,\mathrm{d}t = 0,\\ &\mathrm{d}v_2 + 2\omega v_1 \mathrm{d}t = 0,\\ &d\left(v_3 + \frac{2a}{\chi - 1}\right) = 0, \end{aligned} \tag{4}$$

where $a = \sqrt{\chi(p/\rho)}$ is the sound velocity, T_0 and P_0 are the total temperature and the total pressure, α and γ are the flow angles in the circumferential and meridional directions, respectively.

On the blade surface, because the grid moves with the blade, the normal relative velocity is set to zero:

$$(\boldsymbol{v} - \boldsymbol{w}) \cdot \boldsymbol{n} = 0.$$

The calculation of difference Eq. (2) is reduced to the definition in explicit form of the gasdynamic parameters $\boldsymbol{f}^{n+1}$ at the time $t = t_n + \Delta t$, for gasdynamic parameters at the moment t_n , and values of $(\bar{F}_1, \bar{F}_2, \bar{F}_3)$ calculated with the use of the above formulas.

The time step Δt is constant for all the calculated domain and is defined from the stability condition of the difference scheme for linearized equations system (Chew et al., 1998):

$$\begin{aligned} &\Delta t \leqslant \frac{\tau_x \tau_y \tau_z}{\tau_x \tau_y + \tau_x \tau_z + \tau_y \tau_z},\\ &\tau_i = \frac{h_{i\min}}{\max(v_i + |a|_1 v_i - |a|)} \quad i = x, y, z, \end{aligned}$$

where a is the sound velocity.

2.2. Structural model

The dynamical model of the oscillating blade in linearized formulation is governed by the matrix equation

$$[M]\{\ddot{u}(x,t)\} + [C]\{\dot{u}(x,t)\} + [K]\{u(x,t)\} = \{F\}, \tag{5}$$

where $[M]$, $[C]$, $[K]$ are the mass, mechanical damping and stiffness matrices of the blade, respectively; $u(x,t)$ is the blade displacement, F is the unsteady aerodynamic force vector, which is a function of blade displacement.

The first step in the modal approach consists of solving the problem of the natural mode shapes and eigenvalues without damping and in vacuum. Then, the displacement of each blade can be written as a linear combination of the first N mode shapes with the modal coefficients depending on time:

$$\{u(x,t)\} = [U(x)]\{q(t)\} = \sum_{i=1}^{N} \{U_i(x)\} q_i(t). \tag{6}$$

Here $U_i(x)$ is the displacement vector corresponding to i th mode shape, and $q_i(t)$ is the modal coefficient of ith mode. Substituting (6) into (5) and taking into account the orthogonality property of the mode shapes, Eq. (5) can be written in the form

$$[I]\{\ddot{q}(t)\} + [H]\{\dot{q}(t)\} + [\Omega]\{q(t)\} = \{\lambda(t)\}. \tag{7}$$

Here $[I] = \mathrm{diag}\,(1,1,\ldots 1)$, $[H] = \mathrm{diag}\,(2h_1, 2h_2, \ldots 2h_n)$; $[\Omega] = \mathrm{diag}(\omega_1^2, \omega_2^2, \ldots \omega_i^2)$ are reduced diagonal matrices, ω_i is the i th natural blade frequency, $\{\lambda(t)\}$ is the modal force vector corresponding to the mode shapes, $h_i = 2\omega_i \xi_i$, where ξ_i is the ith modal damping coefficient. Thus, the dynamical problem (5) reduces to a set of decoupled differential equations, relatively to modal coefficients of natural modes:

$$\ddot{q}_i(t) + 2h_i \dot{q}_i(t) + \omega_i^2 q_i(t) = \lambda_i(t), \tag{8}$$

the dimensionality of which is lower by a few orders than problem (5). The equations of motion (8) can be solved using any standard integration method.

The modal forces λ_i are calculated at each iteration with the use of the instantaneous pressure field in the following way:

$$\lambda_i = \frac{\int\int_{\sigma} p \bar{\boldsymbol{U}}_{\boldsymbol{i}} \cdot \bar{\boldsymbol{n}}^{\circ}\, \mathrm{d}\sigma}{\int\int\int_{v} \rho \bar{U}_i^2\, \mathrm{d}v}, \tag{9}$$

where p is the pressure along the blade surface, ρ is the density.

3. Numerical results

The numerical calculations have been carried out for a compressor cascade (the First Standard Configuration) and for a turbine cascade (the Fourth Standard Configuration), to compare with experiments presented by Bolcs and Fransson (1986). The comparison has showed a good agreement between predicted and measured values (Gnesin et al., 2000; Gnesin, 1999).

Below is presented the numerical aeroelasticity analysis for the last stage of a steam turbine with a rotor blade length of 765 mm and with stator-to-rotor blades number ratio of 56:96 (7:12). The calculation was performed for a nominal regime under the gasdynamic parameters.

At turbine stage inlet:

$$P_0 = 12600\,\mathrm{Pa}, \quad T_0 = 323^{\circ}\,\mathrm{K}.$$

At turbine stage outlet:

$$P_2 = 2300\,\mathrm{Pa}.$$

The blade oscillations were computed taking into account the first ten natural modes of oscillations and mechanical damping. The values of the natural frequencies and mechanical damping coefficients are given in Table 1.

The numerical calculations have been made using a computational H-grid with density of $10 \times 24 \times 58$ points per each stator passage and $10 \times 14 \times 58$ grid points for each rotor passage.

The instantaneous distribution of gasdynamic parameters in the axial gap is presented in Fig. 3. The variation of the non-dimensional static pressure ($\bar{p} = p/\boldsymbol{\rho}_* \boldsymbol{a}_*^2$; $\boldsymbol{\rho}_*$ and a_* are the critical density and velocity) is shown in Fig. 3(a), the

relative velocity ($\bar{v} = \sqrt{v_1^2 + v_2^2 + v_3^2}/a_*$) in front of rotor blades in Fig. 3(b), and the angle of the rotor blade entrance velocity in Fig. 3(c). The subscripts $1''$, $2''$, $3''$ correspond to root, middle and peripheral sections, respectively. From this figure we can see that non-uniformity of gas flow displays maximal values in the root section and it decreases in the direction of the peripheral section. The maximal nonuniformity in the static pressure and velocity are about 25% relative to the mean gas flow, and non-uniformity in the flow angle of attack is $-10°–+10°$.

One of the important aspects of stator–rotor interaction is the effect of blade response while taking into account the excitation caused by both the outer flow non-uniformity (the potential non-uniformity and the vorticity wakes behind the stator blade edges which are due to the flow circulation changing in time) and excitation due to blade oscillations.

Table 1
The values of the natural frequencies and mechanical damping coefficients

Mode no.	1	2	3	4	5	6	7	8	9	10
v_i (Hz)	99	160	268	297	398	598	680	862	1040	1124
h_i (Hz)	0.149	0.304	0.62	0.8	1.23	2.1	2.65	3.7	4.89	5.73

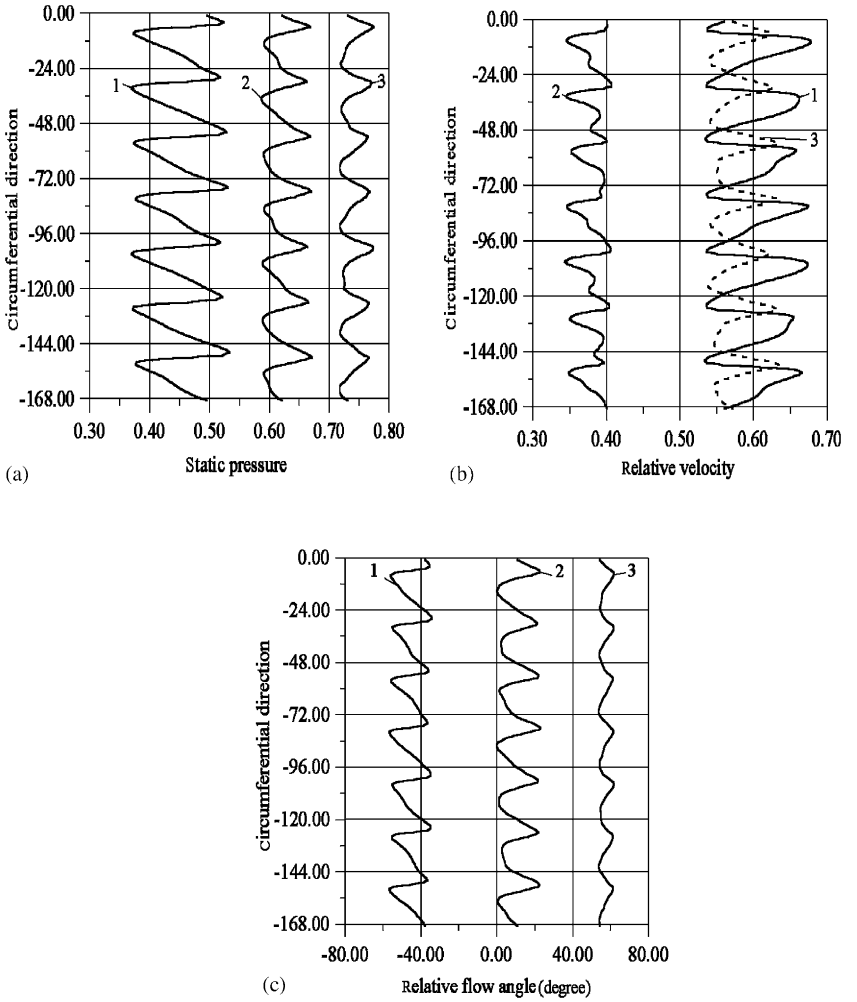

Fig. 3. Gasdynamic parameters distribution in axial gap of the turbine stage without blades oscillations.

In Fig. 4 are shown the graphs of unsteady modal forces corresponding to the firs and second modes of oscillation for the first and fifth blades. The calculation includes two regimes. The first regime ($t = 0$–0.0075 s) involves the calculation of unsteady flow through the turbine stage, while taking into account the rotor-wheel rotation, but without blade oscillations. As the angular rotor velocity v is 50 Hz, the time period corresponding to rotor moving past the zone periodicity (seven stator blade passages, see Fig. 1) is equal to $T_s = \frac{1}{8}(1/v) = 0.0025$ s. As we can see in Fig. 4, it took a time of 0.0075 s (three multiples of T_s) to reach the unsteady periodic solution.

At some point in time, called 'start regime' (for our calculation it corresponds to time instant of 0.0075 s), all blades start to vibrate by the action of the instantaneous forces acting on the blades. Beginning from the start regime, the unsteady phenomena in the turbine stage are the result of continuous force interaction between the gas flow, rotating rotor wheel and oscillating blades. So, it is impossible to separate the unsteady effects caused by external excitation and the unsteady effects due to blade oscillations.

In Fig. 5 are presented in enlarged scale the graphs of the modal forces corresponding to the first mode for the first and fifth rotor blades at the beginning of transient ($t = 0.005$–0.0125 s) and at the end of the seventh full rotor revolution ($t = 0.141$–0.149 s). In accordance with stator-to-rotor blades ratio $z_s : z_r = 7 : 12$, the load phase lag for ith blade compared to the first one is $2\pi(i-1)z_s/z_r$ or $7\pi(i-1)/6$. As we can observe from the graphs, the load phase shift does not depend on the blade oscillation, it is defined only with stator-to-rotor blades ratio and it is equal to $2\pi/3$ for the fifth blade.

It is interesting to note the following:

(i) the unsteady force variation includes a high-frequency harmonic ($v = 2800$ Hz) corresponding to the rotor moving past one stator-blade pitch and a spectrum of low frequencies (see Fig. 4);
(ii) the force variation is an aperiodic function of time, or so-called "almost periodic function" with period approaching to infinity;
(iii) the forces acting on the different blades differ from one another.

The amplitude-frequency characteristics for the unsteady forces corresponding to the first, second, third and eighth natural modes are shown in Fig. 6.

As seen from the graphs, the spectra of all modes include high-frequency harmonics (2800, 5600 Hz) corresponding to the pitch non-uniformity, and low-frequency harmonics due to the non-uniformity along a full circle caused by blade oscillations.

The blade moving is presented in Figs. 7 and 8 in the form of modal coefficient dependence in time. Fig. 7 demonstrates the modal coefficients, corresponding to the first (Fig. 7(a)) and second (Fig. 7(b)) modes for the first and fifth blades versus time.

In Fig. 8 shows the blade motion in the eighth mode. From these figures the following should be noted:

(i) the blade oscillations in the first mode pass to an auto-oscillation regime with a frequency which is smaller than the natural one (see dotted line in Fig. (7a));
(ii) the logarithmic decrement of oscillations increases with the mode number;
(iii) the blade oscillations in low modes do not contain high frequencies, while the oscillations in the eighth mode include both low and high frequencies (Fig. 8);
(iv) the blade oscillations phase shift depends not only on the stator-to-rotor blades ratio but also on the natural oscillations frequency.

The amplitude-frequency characteristics of blade oscillations for the first, second, third and eighth modes are presented in Fig. 9. As we can see, the blade oscillations in the ith mode are at a frequency, which is less than the natural frequency of oscillations. The difference in the frequencies is about 20–30% from the natural one.

In Figs. 10–12 are represented the computational results for the same turbine last stage in an off-design regime, which is characterized by a raised back pressure and non-uniformity in pressure distribution along the pitchwise direction. It was accepted that the sinusoidal law of pressure change from blade to blade applies, as shown in Fig. 10. The integers on the abscissa correspond to rotor blade number (the rotor wheel includes 96 blades). Fig. 11(a) shows the graphs of the unsteady modal forces corresponding to the first and second modes for the first blade during a full rotor revolution. In Figs. 11(b,c) we can observe that the amplitude-frequency characteristics for the first and second modes include a high-frequency harmonic ($vz_3 = 2800$ Hz) corresponding to the rotor moving past one stator-blade pitch, and a low-frequency force component (50 Hz) corresponding to the rotor rotation frequency. Moreover, the value of the high-frequency force component acting on the blade varies with the blade rotation, but its amplitude is significantly smaller than the amplitude of low-frequency unsteady force.

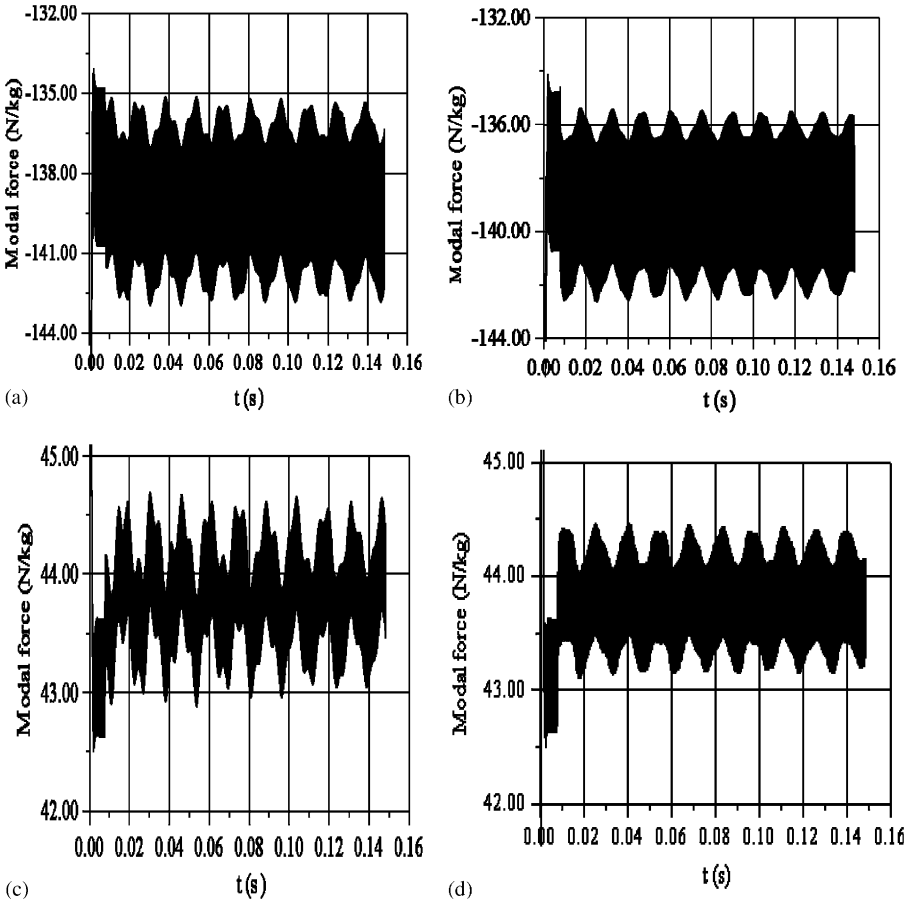

Fig. 4. The unsteady force variation while taking into account the blade oscillations: (a) and (b) first and fifth blades, first mode; (c) and (d) first and fifth blades, second mode.

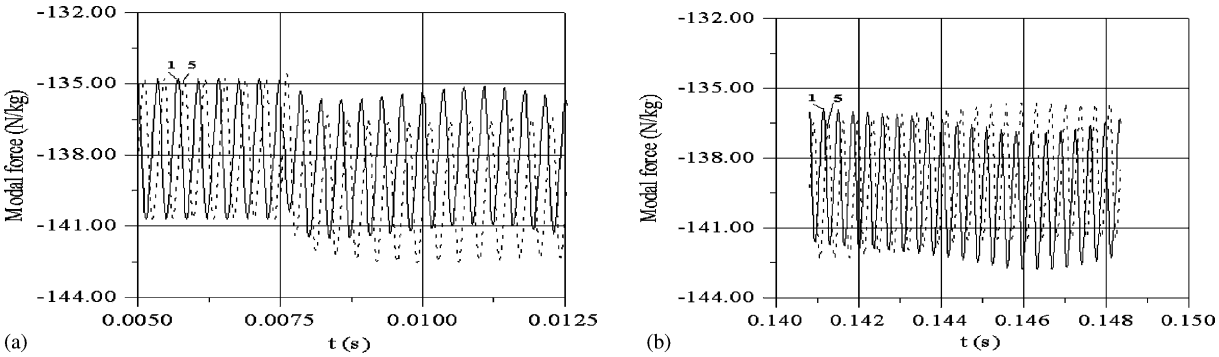

Fig. 5. The first mode unsteady force variation for the first and fifth blades while taking into account the blade oscillations, for (a) the beginning of the transient and (b) the end of the transient.

The blade motion in the form of the modal coefficients variation in time for the first and second modes of the first blade is presented in Fig. 12.

As we can see, the blade oscillations are stable oscillations, including mainly the first natural mode of oscillations (the integer in Fig. 12(a) correspond to mode numbers). Fig. 12(b) shows the amplitude-frequency spectrum of the blade

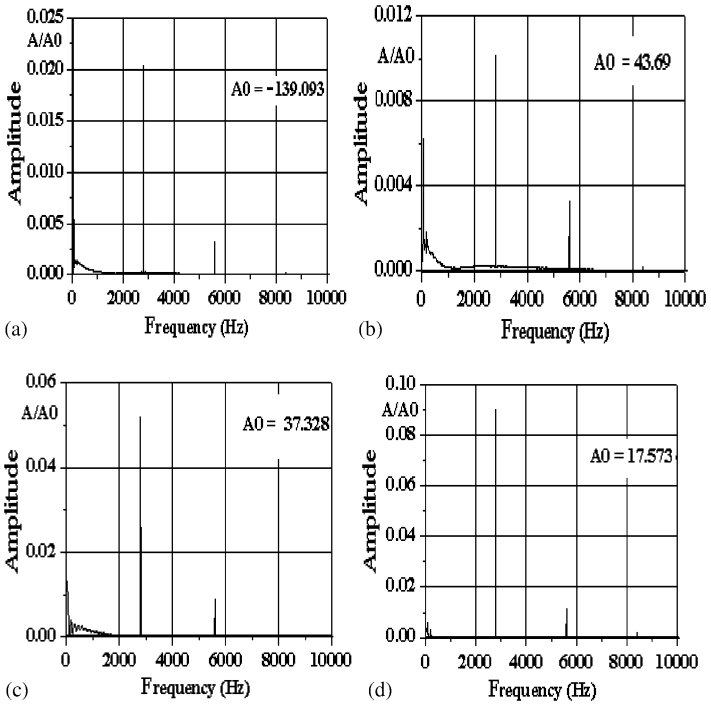

Fig. 6. Amplitude-frequency characteristics for unsteady aerodynamical forces acting on the first blade: (a) first mode, (b) second mode, (c) third mode, (d) eighth mode.

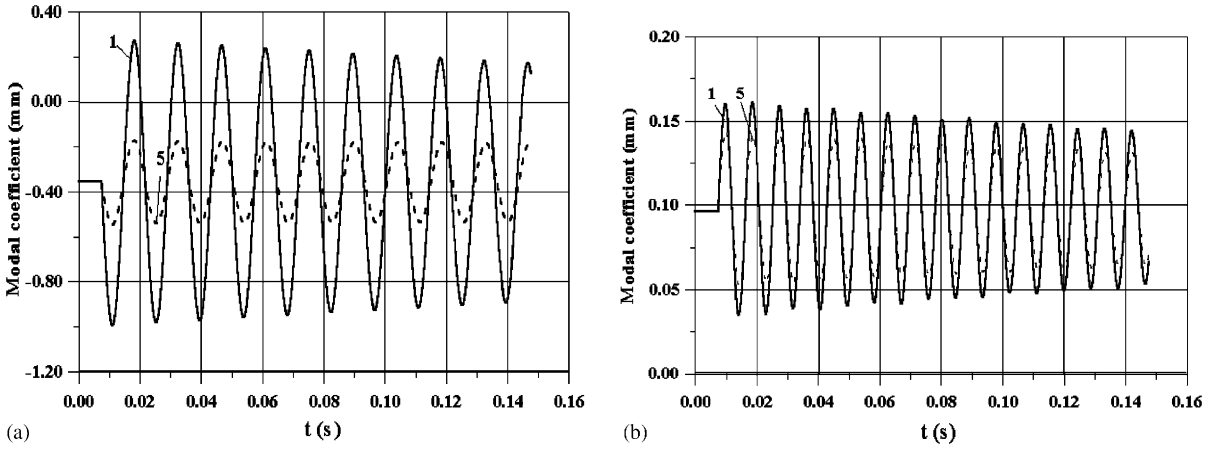

Fig. 7. The modal coefficient for the first and fifth blades versus time: (a) first mode, (b) second mode.

vibration in the first mode. The spectrum includes the blade oscillation frequencies close to their natural ones (not multiples of rotation frequency) and frequencies caused by low-frequency forced loads, which are multiples of the rotor rotation frequency.

4. Conclusions

A partially integrated method is adopted for the solution of the coupled aerodynamic-structural problem of 3-D flow through a turbine stage while taking into account rotor blade oscillations.

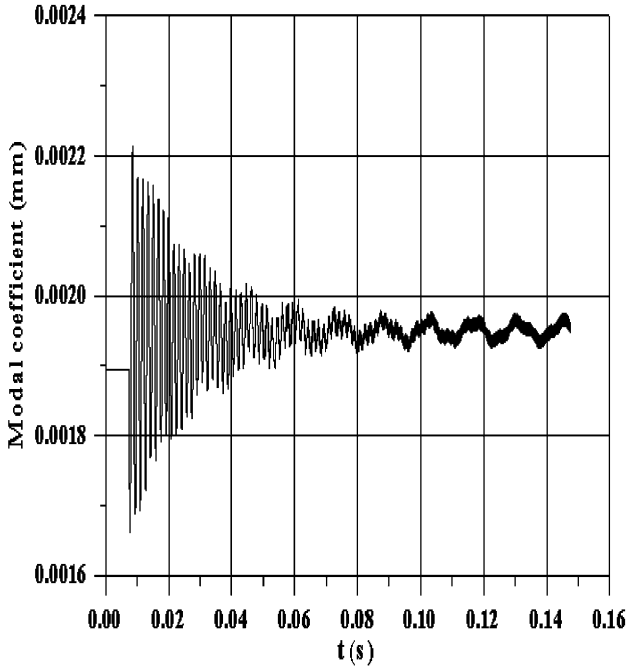

Fig. 8. The eighth mode modal coefficient for the first blade.

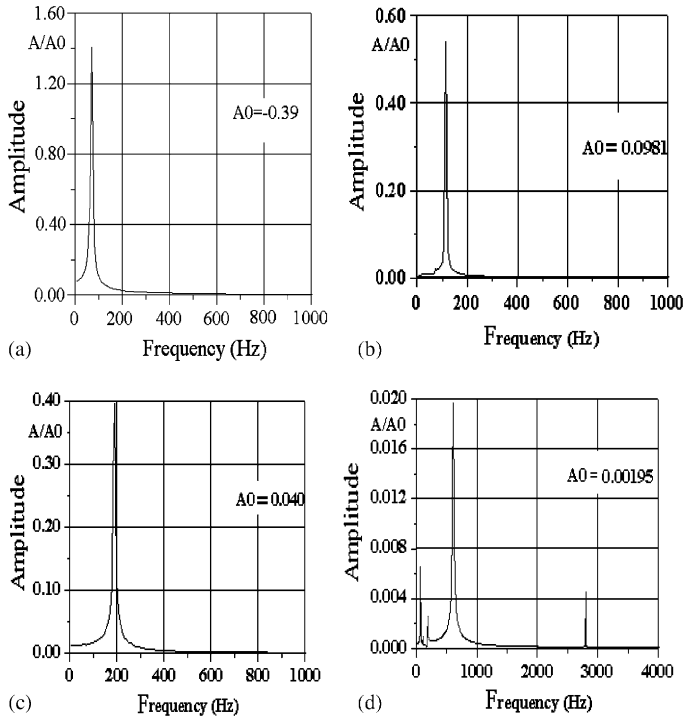

Fig. 9. Amplitude-frequency characteristics for the first blade motion: (a) first mode, (b) second mode, (c) third mode, (d) eighth mode.

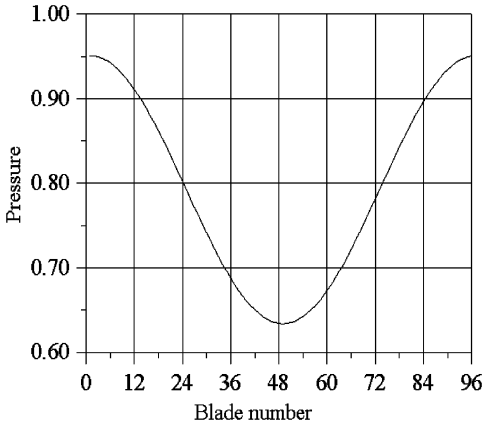

Fig. 10. The back-pressure distribution at the exit of the stage under off-design conditions.

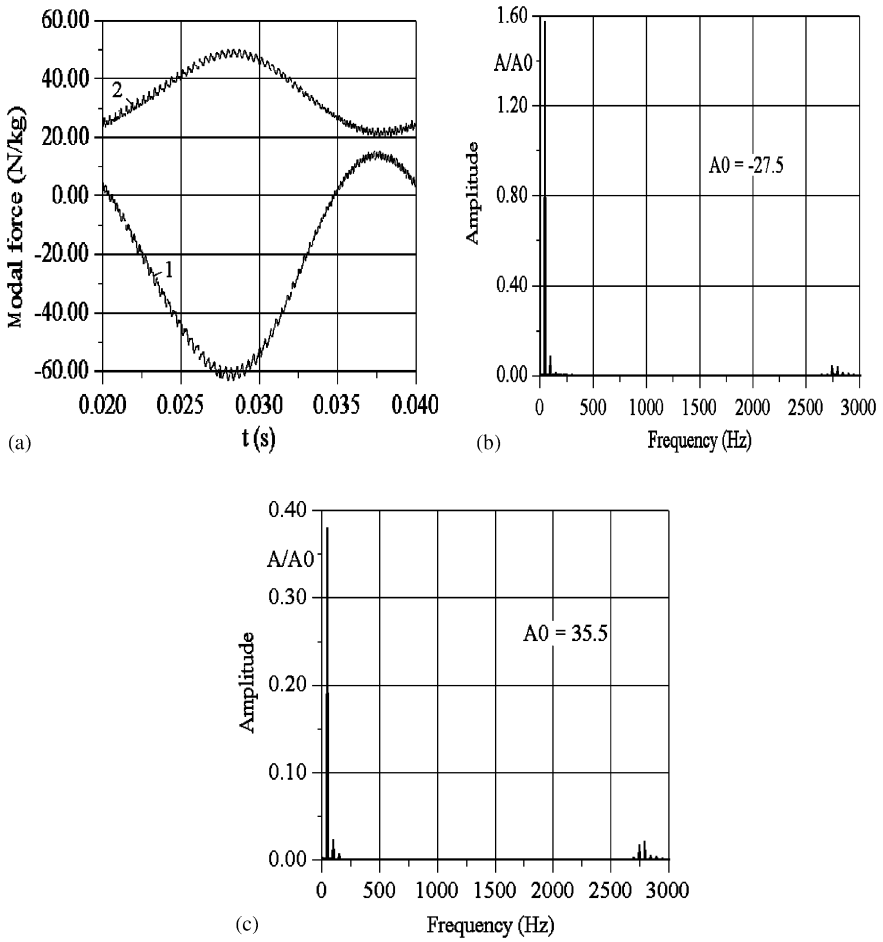

Fig. 11. The modal force variation during a full rotor revolution.

The mutual influence of both outer flow non-uniformity and non-stationarity caused by blade oscillation were investigated.

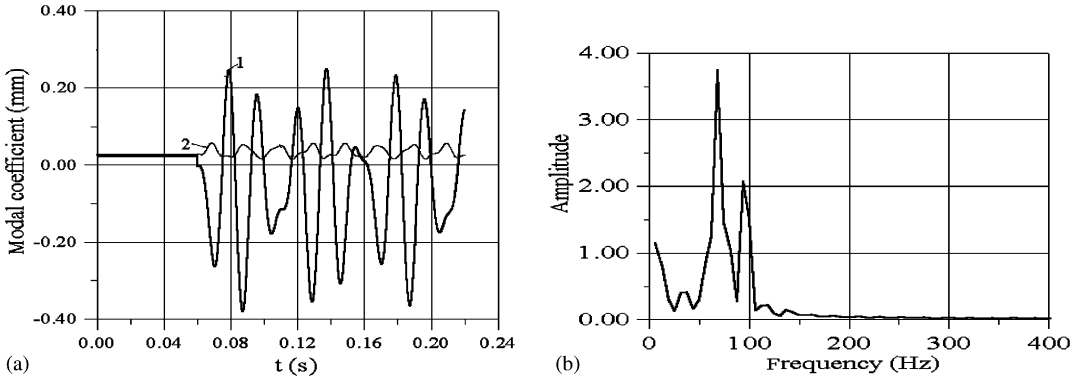

Fig. 12. The blade oscillations under off-design conditions.

It has been shown that the amplitude-frequency spectrum of blade oscillations contains harmonics with high frequencies and low frequencies, which are not multiples of the rotation frequency.

Acknowledgements

This research was supported in part by the National Academy of Sciences of Ukraine under contract 14 and by the Polish grant from the State Committee for Scientific Research, Warsaw, No. 0826/T07/2003/25.

References

Bakhle, M.A., Reddy, T.S.R., Keith, T.G., 1992. Time domain flutter analysis of cascades using a full-potential solver. AIAA Journal 30 (1), 163.

Bolcs, A., Fransson, T.H., 1986. Aeroelasticity in turbomachines: comparison of theoretical and experimental cascade results, Communication du LTAT-EPFL, Switzerland, No. 13, p. 174.

Chew, J.W., Marshall, J.G., Vahdati, M., Imregun, M., 1998. Part-speed flutter analysis of a wide-chord fan blade. In: Fransson, T.H. (Ed.), Unsteady Aerodynamics and Aeroelasticity of Turbomachines. Kluwer Academic Publishers, Dordrecht, pp. 707–724.

Gnesin, V.I., 1982. The calculation of three-dimensional transonic gas flow through the axial turbine stage. News of USSR Academy of Science, Gas and Fluid Mechanics, Moscow, No. 6, pp. 138–146 (in Russian).

Gnesin, V.I., 1999. A numerical study of 3-D flutter in turbomachines using fluid–structure coupled method. Engineering Mechanics 6 (4/5), 253–267.

Gnesin, V.I., Kolodyazhnaya, L.V., 1999. Numerical modelling of aeroelastic behaviour for oscillating turbine blade row in 3-D transonic ideal flow. Problems in Machinery Engineering 1 (2), 65–76.

Gnesin, V., Rzadkowski, R., Kolodyazhnaya, L., 2000. A coupled fluid–structure analysis for 3-D flutter in turbomachines. ASME 2000-GT-380, International Gas Turbine and Aeroengine Congress, Munich, Germany, 8pp.

Godunov, S.K., Zabrodin, A.V., Ivanov, M.Ya., Krajko, A.N., Prokopov, G.P., 1976. Numerical Solution of Multidimensional Problems in Gasdynamics. Nauka, Moscow (in Russian).

Koya, M., Kotake, S., 1985. Numerical analysis of fully three-dimensional periodic flows through a turbine stage. ASME Journal of Engineering for Gas Turbines and Power 107.

Rao, K., Delancy, R., 1990. Investigation of unsteady flow through transonic turbine stages. AIAA Paper 90-2408/2409.

Yershov, S.V., Rusanov, A.V., Shapochka, A.Y., 2001. 3D viscous transonic turbomachinery flows: numerical simulation and optimization using code FlowER. Proceedings of the 5th ISAIF, September 4–7, Gdansk, Poland, pp. 229–236.